JOURNAL OF MATERIALS SCIENCE 8 (1973) 233–244

The elastic constants of carbon-fibre composites

P. R. GOGGIN
Metallurgy Division, UKAEA Research Group, Atomic Research Establishment, Harwell, Berks, UK

Data on the elastic constants of carbon-fibre composites are presented. It is shown that provided the elastic constants of both the fibre and the matrix are known it is possible to predict the elastic constants of the composite parallel to the fibre axis using either the reduced equations of Halpin and Tsai, based on a self-consistent model, or the exact calculations of Heaton. The properties of the composite perpendicular to the fibres cannot be explained on the basis of the theoretical models considered.

1. Introduction

In order to predict the behaviour of a composite material stressed within its linear elastic range it is necessary to know the elestic constants and forces applied. The elastic constants of a range of composites manufactured from various resin systems and from two types of carbon fibre, laid axially, have been determined. The values obtained have been compared with the values predicted from the properties of the matrix materials and the carbon fibres. Before describing the experimental and analytical methods used some definition of the elastic constants and their relation to physically measured properties is necessary.

Provided the fibres are distributed throughout the matrix so that the material is isotropic perpendicular to the fibres, then such a material has cylindrical or hexagonal symmetry. In order to describe its behaviour it is necessary to know five independent elastic constants. Using the standard notation of Kittel [1] these constants are denoted by:

$$S_{11}, S_{12}, S_{13}, S_{33}, S_{44}$$

S_{11} relates the strain perpendicular to the fibres to a stress applied in the same direction; S_{33} relates the strain parallel to the fibres to a stress applied in this direction; S_{12} relates the strain perpendicular to the fibres to a stress applied perpendicular to the strain; S_{13} relates the strain perpendicular to the fibres to a stress applied parallel to them; S_{44} relates the shear strain about an axis perpendicular to the fibres to a couple about the same axis.

The measured laboratory constants are the Young's moduli parallel and perpendicular to the fibre axis, the torsional rigidity parallel and perpendicular to the fibre axis, and the longitudinal and transverse Poisson's ratios. These quantities are denoted by:

$$E_\parallel, E_\perp, G_\parallel, G_\perp, \gamma_\parallel \text{ and } \gamma_\perp$$

They are related to the elastic constants by the following equations

$$E_\parallel = 1/S_{33} \quad (1)$$

$$E_\perp = 1/S_{11} \quad (2)$$

$$G_\parallel = \frac{1}{S_{44}} = C_{44} \quad (3)$$

$$\gamma_\parallel = S_{13}/S_{33} \quad (4)$$

$$\gamma_\perp = S_{12}/S_{11} \quad (5)$$

The elastic constants S_{11}, S_{12}, S_{13}, S_{33} and S_{44} can be calculated directly from the measured laboratory constants using the relations given in Equations 1 to 5. The remaining constant, S_{66}, can be determined either from the relationship $S_{66} = 2(S_{11} - S_{12})$ or from the measurement of the torsional rigidity, $G_\perp$, perpendicular to the fibres. $G_\perp$ depends on C_{44} and C_{66}. For specimens with circular section

$$G_\perp = \tfrac{1}{2}(C_{44} + C_{66}) \quad (6)$$

For specimens with rectangular section the relationship is more complex. According to Love [4] the torque on a sample of rectangular section is given by

$$M_t = \theta C_{44} a^3 b \left\{ \frac{16}{3} - \frac{a}{b} \sqrt{\frac{C_{44}}{C_{66}}} \left(\frac{4}{\pi}\right)^5 \sum_{n=0}^{\infty} \frac{1}{(2n+1)^5} \tanh \left[\frac{(2n+1)\pi b}{2a} \sqrt{\frac{C_{44}}{C_{66}}} \right] \right\} \quad (7)$$

where n may be regarded as analogous to mode. As C_{44} is known C_{66} can be calculated from Equation 7 by an iterative process.

2. Experimental techniques

2.1. Manufacture of specimens

The samples used were produced in two basic forms. The first was a cast bar about 30 cm long, 1.25 cm wide, and 0.25 cm thick. Most of the bars were produced by hand-laying a known weight of fibre into a mould, vacuum impregnating with resin and then pressing and curing. Some bars were, however, produced by a filament-winding technique in which the fibres were wound into special moulds under tension. A number of different fibre – volume loadings was used for each type of fibre in the various resin systems.

Blocks of composites each 25 cm square by 0.6 cm thick were also produced by hand-laying fibre in a mould and vacuum-impregnating with resin. Again a variety of volume-loadings was produced for each type of fibre and resin system. Blocks of pure resin were also cast for each system used. Six samples were then cut from each of the blocks. Three were cut parallel to the fibre axis and three perpendicular to it. The samples were each $10 \times 0.8 \times 0.5$ cm. Considerable difficulty was found in machining samples perpendicular to the fibre direction and some samples had to be rejected owing to distortion.

2.2. Measurement of volume fraction of fibre

The volume fraction of fibre in the long bars was estimated from the dimensions of the bars, the weight of fibre used and the density of the fibre. From the density of the pure resin it was also possible to calculate the void volume in each of the long bars. In the principal system studied this was 1 to 2% but was somewhat higher for some of the other resin systems.

In the case of the samples cut from the blocks the volume fraction of fibre was estimated from the density of the individual samples.

2.3. Dynamic Young's modulus

The dynamic Young's modulus was measured by a Förster resonant bar technique in which transverse modes were excited in the specimen. With the long bars it was possible to excite up to six modes in which the direction of vibration was perpendicular to the wide face of the bar. It was found that the apparent Young's modulus decreased with increasing mode number. This effect is due to the increased importance of correction for shear deformation and rotational inertia as the effective aspect ratio of the specimen decreases. These correction factors are well known for isotropic homogeneous materials and have been summarized by Ramsden [2]. The appropriate values for samples with similar dimensions to those used in these experiments are given in Table I. These are for homogeneous isotropic materials and the corrections will be larger for anisotropic materials. The actual frequency ratios for different modes were found to be very similar to the theoretical frequency ratios, predicted for homogeneous isotropic materials.

The dynamic moduli of the short bars cut both parallel and perpendicular to the fibre direction were measured on the same apparatus. In the case of bars cut parallel to the fibres it was possible to excite only one or two modes with the wide face either vertical or horizontal. For bars cut perpendicular to the fibres three modes could be found in each case. The results quoted are those calculated from the first mode since this will be the most accurate and will be less sensitive to local variations in fibre concentration.

2.4. Static Young's modulus

The static Young's modulus was measured by a three-point bending beam method on both the long and the short bars. The determination of the Young's modulus of materials with a high modulus (say 20 to 30 $\times$ 10^6 psi) from a three-point bend test is not straightforward owing to the interfering effects of deflection due to shear, bedding down at the loading points and machine softness. This is illustrated in Fig. 1, which shows the apparent Young's modulus of composite bars with the fibre laid parallel to the bar as a function of the ratio of separation of outer supports to specimen thickness. In the case of fibres cut perpendicular to the fibre direction, for which the modulus is much lower, the apparent modulus is almost independent of the gauge length used.

TABLE I Correction constants for the vibrational Young's modulus for different mode numbers and aspect ratios

Aspect ratio	Mode					
	1	2	3	4	5	6
12:1	1.043	1.122	1.24	1.41		
20:1	1.017	1.046	1.091	1.151	1.187	1.268
100:1	1.004	1.010	1.020	1.032	1.044	1.060

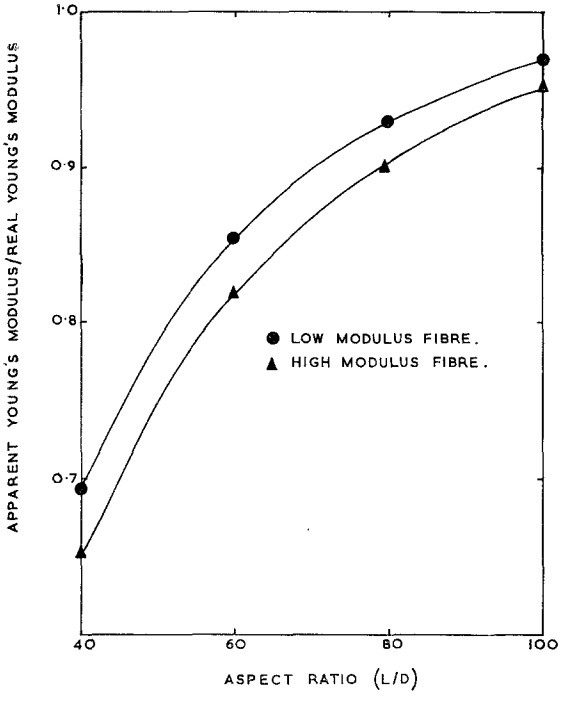

Figure 1 The ratio of apparent Young's modulus to real Young's modulus as a function of aspect ratio of the test bar.

The true Young's modulus was obtained from data of this type in the following manner. The observed deflection of a beam supported at its ends and loaded at its centre point is given by:

$$\delta_0 = PL^3 + QL + R$$

where P is a constant depending on the Young's modulus, applied load and cross section of the sample; Q is a constant depending on the shear modulus, applied load and cross section of the sample; R is a constant depending on the machine softness and depression at loading points and applied load; L is gauge length of sample.

If δ_0 is measured as a function of gauge length for the same maximum load then P can be obtained by the method of least squares and hence the true modulus can be evaluated.

All the long bars and the short bars cut perpendicular to the fibre direction showed a linear elastic deformation. In some of the short bars cut parallel to the fibres the stress-strain diagram showed considerable curvature and it was not possible to analyse the data.

2.5. Tensile Young's modulus and Poisson's ratio

The Young's modulus of the long bars was measured in tension and the strain monitored by foil strain gauges to obtain values for both the Young's modulus and the Poisson's ratio. Six strain gauges were mounted at the middle of the wide faces of the bars. Two pairs were used to measure tensile strain and the other pair to measure lateral strain. One of each pair was mounted on each wide face of the bar. The gauges were monitored independently and strains noted as a function of applied load. With the arrangement of gauges used it was possible to check that the specimen was under true tension and that no bending took place. The maximum stress applied was about 25% of the UTS of the bars. The samples showed perfectly linear elasticity in the strain range studied (2×10^{-6} to 1×10^{-3}). The Young's modulus obtained by this method agreed closely with the values obtained on the same samples using the bending beam method.

2.6 Torsional rigidity

The torsional rigidity both parallel and perpendicular to the fibres was measured on the short bars. Samples were mounted in an apparatus specially constructed to allow a torque to be applied without bending the samples. Mirrors were mounted on the face of the specimens and the deflection of the gauge length measured by lamp and scale technique. The deflection was measured as a function of torque applied both clockwise and anticlockwise. The torsional

rigidity was taken as the ratio of maximum stress over maximum strain. The computation of the true shear modulus on rectangular specimens presents some difficulties. For the specimens cut parallel to the fibres there is only one rigidity modulus involved and it can be shown that

$$G_{\parallel} = \frac{WR}{w\theta a^3 b}$$

where $G_{\parallel}$ = rigidity modulus parallel to the fibres; W = load applied in dynes; R = radius about which load is applieds; θ = angle of twist per unit length of sample; b = width of specimen; a = thickness of specimen; K = constant depending on a and b.

Timoshenko and Goodier [3] show that

$$K = \tfrac{1}{3}\left[1 - \frac{192}{5}\frac{a}{b}\sum_{n=0}^{\infty}\frac{1}{(2n+1)^2}\tanh\frac{b(2n+1)}{2a}\right]$$

where n is analogous to the mode.

This is rapidly convergent and can easily be computed for each specimen from its dimensions. Hence $G_{\parallel}$ can be evaluated and, since $G_{\parallel} = 1/S_{44}$, S_{44} can be computed.

The perpendicular torsional rigidity modulus was obtained in a similar manner.

3. Results

3.1. Fibre properties

Batches of fibre from which the composites were manufactured have been tested by the normal methods. The results are shown in Table II.

3.2. Properties of matrix materials

The properties of the resin systems used were measured on samples machined from cast blocks. These materials are isotropic and their mechanical behaviour can be described by two elastic constants. The properties are summarized in Table III.

3.3. Young's modulus

Fig. 2 shows the Young's modulus parallel to the fibre direction as a function of fibre volume fraction for type 1 fibre in resin system A. Results for both hand-laid and tension-wound bars are shown. Data for hand-laid bars using the other resin systems were similar to the results obtained on resin system A. The results from the tension-wound bars were considerably higher than from the hand-laid bars and were close to the moduli predicted from the volume fraction of fibres and law of mixtures. This is due to the better fibre alignment achieved with tension winding.

Fig. 3 shows the Young's modulus parallel to the fibres for type 2 fibres in resin system A as a function of fibre volume fraction. The data was in general within 10% of the results predicted by the law of mixtures. Similar results were obtained with the other resin systems.

TABLE II Measured properties of the fibres used in the manufacture of the composites

Type	Young's modulus		Tensile strength		Diameter (μm)
	($\times 10^{-6}$ psi)	(GNm^{-2})	($\times 10^{-3}$ psi)	(GNm^{-2})	
1	56.9 ± 1.0	395 ± 8	224 ± 12	1.53 ± 0.08	7.9 ± 0.1
2	33.2 ± 1.2	230 ± 9	285 ± 30	1.96 ± 0.2	8.6 ± 0.3

TABLE III Properties of the various resin systems

Resin	Young's modulus		Shear modulus		Poisson's ratio
	($\times 10^{-6}$ psi)	(GNm^{-2})	($\times 10^{-6}$ psi)	(GNm^{-2})	
A	0.56	3.9	0.21	1.4	0.33
AV1	0.53	3.7	0.21	1.4	0.30
AV2	0.48	3.3	0.18	1.2	0.32
AV3	0.51	3.5	0.19	1.3	0.31
B	0.57	4.0	0.22	1.5	0.31
C	0.86	6.0	0.32	2.2	0.36

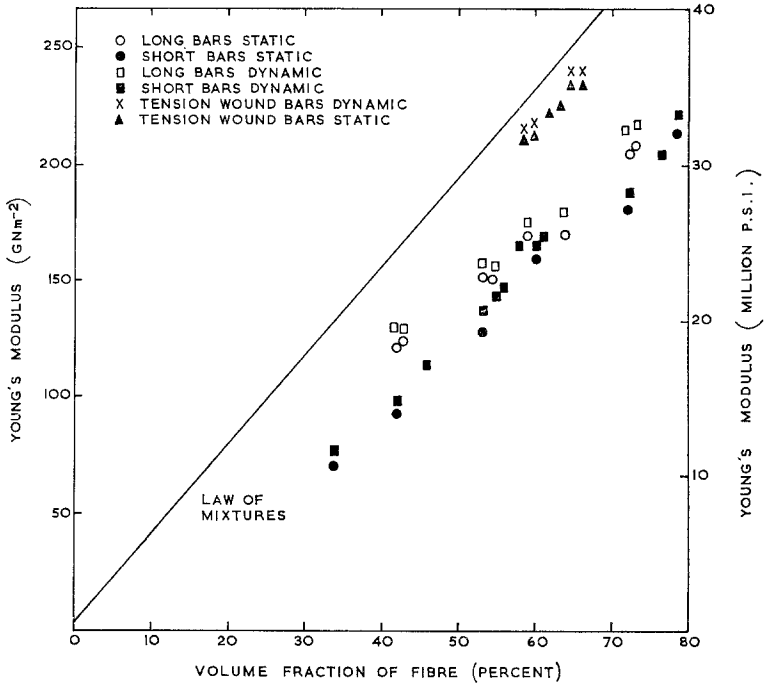

Figure 2 The Young's modulus parallel to the fibres as a function of volume fraction of type 1 fibre in resin system A.

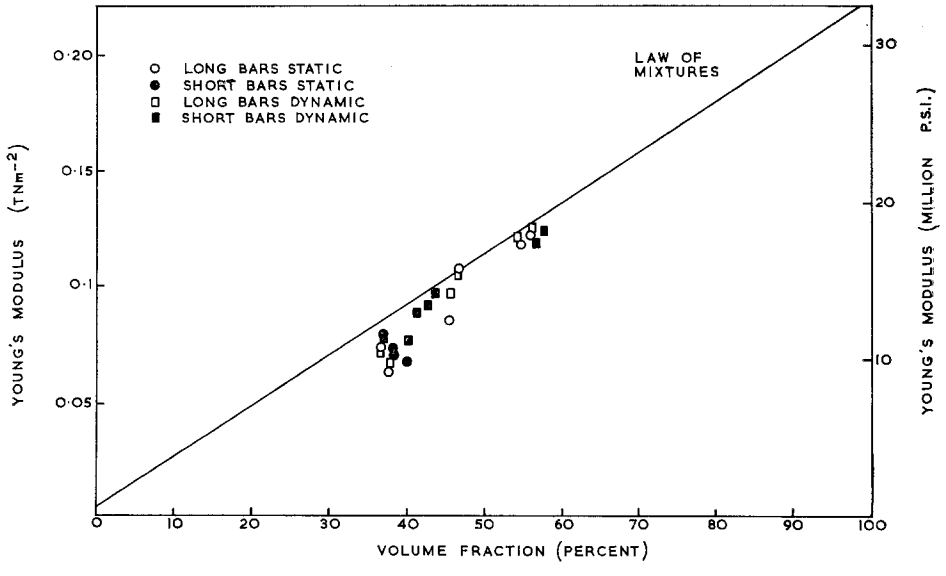

Figure 3 The Young's modulus parallel to the fibres as a function of volume fraction of type 2 fibre in resin system A.

The Young's modulus perpendicular to the fibres is shown in the next figure as a function of volume fraction of fibre for both type 1 and type 2 fibre in resin system A. It should be noted that the type 2 fibres give a higher transverse modulus than the type 1 fibres. This probably reflects the more anisotropic nature of the type 1 fibre.

3.4. Torsional rigidity

The torsional rigidity parallel and perpendicular

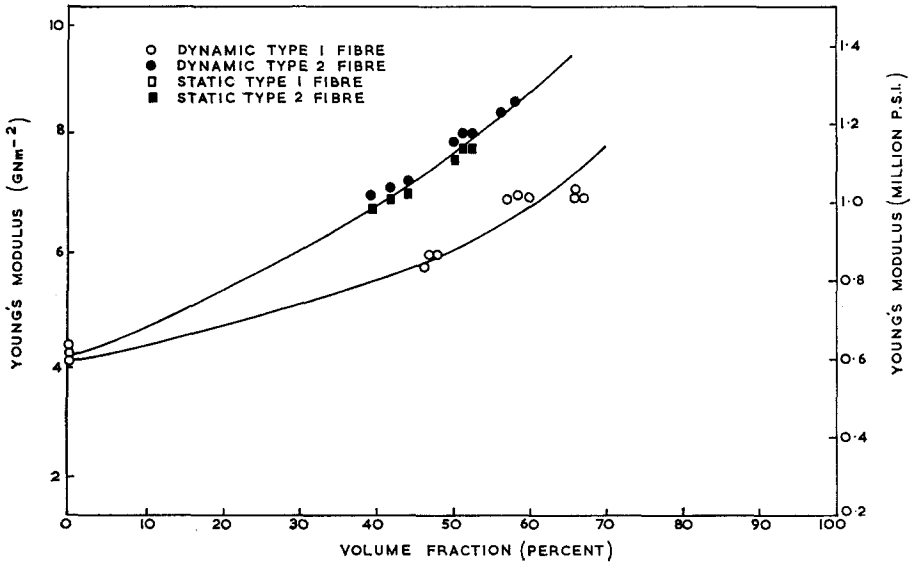

Figure 4 The Young's modulus perpendicular to the fibres as a function of volume fraction of both type 1 and type 2 fibres in resin system A.

to the fibre for both type 1 and type 2 fibre in resin systems A and C is shown in Fig. 5. Resin system C had a higher Young's modulus and rigidity modulus than the other systems examined and this is reflected in the higher rigidity modulus of the composites. It should be noted that parallel to the fibres (i.e. twisting about the fibre axis) the rigidity modulus is independent of the type of fibre used. The torsional rigidity perpendicular to the fibres is however sensitive to the properties of the fibre used and is higher for type 2 fibres than for type 1 fibres.

3.5. Poisson's ratio

The longitudinal and transverse Poisson's ratios are shown in Fig. 6 as a function of volume

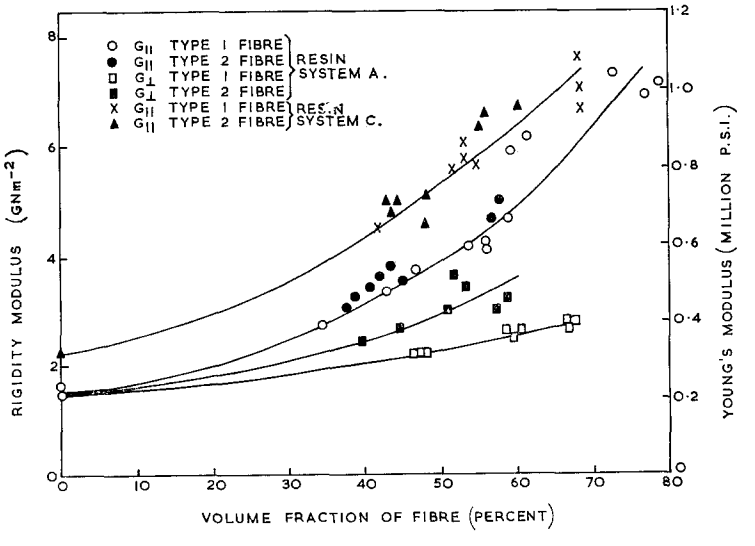

Figure 5 Rigidity modulus as a function of volume fraction of type 1 and type 2 fibre in both resin system A and C.

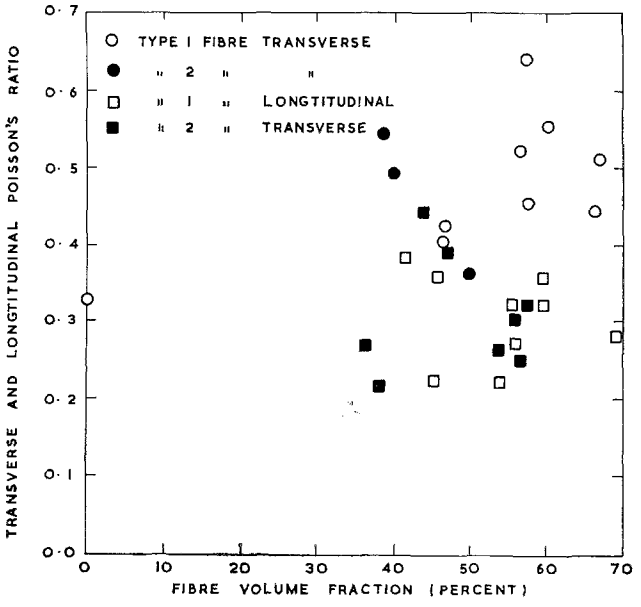

Figure 6 Longitudinal and transverse Poisson's ratios as a function of volume fraction of both type 1 and type 2 fibres in resin system A.

loading of both type 1 and type 2 fibre. There was considerable scatter in the data but the mean longitudinal value for both types of fibre was similar to that of pure resin (i.e. about 0.3) while the mean transverse value for type 1 fibre composites was 0.47 and for type 2 fibres for composites 0.52. These values are significantly higher than the Poisson's ratio of the pure resin.

4. Discussion

The elastic constants of a unidirectional composite material have been calculated theoretically by a number of people. The method of approach varies from netting analysis to complex statistical methods. However, in every case, certain basic assumptions are made about the composite. These are, 1, the composite is macroscopically homogeneous and linearly elastic; 2, the fibres and matrix are independently homogeneous and linearly elastic; 3, the matrix and fibres are free of voids and flaws; 4, the bonding between the fibres and the matrix is perfect and there is no transition region; 5, the fibres are regularly spaced and well aligned.

Several different approaches have been used in the many theoretical calculations. A review of these is given elsewhere [5]. Only the work of Heaton [6, 7] and Halpin and Tsai [8] can be directly applied to the present data.

Halpin and Tsai have examined the calculations and have shown that the various results can be reduced to an approximate form which gives good agreement with the exact calculations.

The approximate solutions are given by

(*a*) for longitudinal tensile properties

$$E_{33} = E_f V_f + E_m V_m$$

$$\gamma_{13} = \gamma_f V_f + \gamma_m V_m ,$$

(*b*) for transverse and shear properties

$$\frac{\bar{P}}{P_m} = \frac{(1 + AB\,V_f)}{(1 = B\,V_f)}$$

where $B = (P_f/P_m - 1)/(P_f/P_m + A)$; $\bar{P}$ = composite modulus; P_m = corresponding matrix modulus; P_f = corresponding fibre modulus; A = reinforcement factor which depends on boundary conditions.

They found that for the prediction of longitudinal shear the best results were obtained for $A = 1$, while for transverse modulus $A = 2$ gave the best results. These calculations, however, all suffer from the drawback that they assume the fibre is isotropic.

Heaton has calculated the elastic constants for a unidirectional composite for both isotropic and anisotropic fibres. His calculations for the isotropic fibre composite agree very closely with the

others. For the anisotropic fibre composite he showed that at intermediate loadings the transverse properties of the composite are determined mainly by the properties of the matrix materials. At higher loadings the anisotropic nature of the fibre is important and transverse reinforcement is considerably less than would be obtained from isotropic fibres. His numerical results for composites made with anisotropic fibres are for type 1 carbon fibres only.

Comparison may now be made between the experimental results and theoretical results based on calculations using the Halpin-Tsai equations or the exact calculations in Heaton's second paper. The assumed fibre moduli are shown in Table IV.

In both theoretical models the Young's modulus predicted parallel to the fibres is within 1% of the value based on the law of mixtures. It should be pointed out that all in the models examined the Young's modulus parallel to the fibres reduced to a uniform strain calculation. It has been shown experimentally that provided care is taken to ensure good alignment of the fibres in the composite then the predicted modulus can be achieved. In the case of hand-laid composites the modulus can be as much as 25% lower than predicted for type 1 fibre and 20% lower than predicted for type 2 fibre. Cook [9], has calculated the effect of imperfect fibre orientation on the elastic constants of composites. This work suggests that if the root mean square fibre scatter was of the order of 10° then the loss in modulus for type 1 fibre would be 25% and for type 2 fibre would be about 15%. Measurements by Egelstaff [10], on composites used in this experiment gave half-widths to the distribution of fibre orientation of between 10 and 20°. This implies a root mean square fibre scatter of about 10° and this is sufficient to explain the observed short fall in the Young's modulus.

The theoretical data and experimental data for the longitudinal shear modulus for both type 1 and type 2 fibre composites are shown in Fig. 7. The longitudinal shear modulus is the only case where it seems appropriate to assume uniform stress in calculating the modulus. However, this gives an answer which is lower than that observed experimentally. Thus at 50% volume fraction of fibre the predicted shear modulus is 2.46 GNm^{-2} whereas the measured value is 3.8 GNm^{-2} and at 70% volume fraction of fibre the predicted value is 4.0 GNm^{-2} while the measured value is 6.8 GNm^{-2}. The calculations based on the reduced equations of Halpin and Tsai give very similar results to the exact calculations by Heaton. The prediction of both the trend and the actual experimental values is very satisfactory for both models.

The data for the transverse shear modulus (C_{66}) are shown in Fig. 8. It should be pointed out that for hexagonal symmetry $C_{66} = \frac{1}{2}(C_{11} - C_{12})$ or $S_{66} = 2(S_{11} - S_{12})$. Both theoretical calculations predict values that are much lower than those recorded experimentally if the assumed fibre elastic constants are used. This implies

TABLE IV Measured and assumed elastic constants of carbon fibres

(*a*) Engineering constants

Modulus	Type 1	Type 2
E_{33} (Longitudinal Young's modulus)*	55×10^6 psi	33×10^6 psi
E_{11} (Transverse Young's modulus)	4×10^6 psi	4×10^6 psi
G_{44} (Longitudinal shear modulus)*	3.8×10^6 psi	3.8×10^6 psi
μ_{13} (Longitudinal Poisson's ratio)	0.5	0.5
μ_{12} (Transverse Poisson's ratio)	0.28	0.28

(*b*) Compliance moduli (in units of $TN^{-1}\,m^2$

Modulus	Type 1	Type 2
S_{33}*	2.6	4.7
S_{11}	36.3	36
S_{44}*	38.3	38
S_{12}	− 10.2	− 10.2
S_{13}	− 1.3	− 2.4

*Measured values.

either that the models fall down in the prediction of this modulus, or that the assumed fibre elastic constants are wrong, or that there is some error in the extraction of the value of S_{66} from the measurement of the torsional rigidity perpendicular to the fibre.

Measurements of S_{11} and S_{12} by strain gauges confirm the values of S_{66} obtained from the

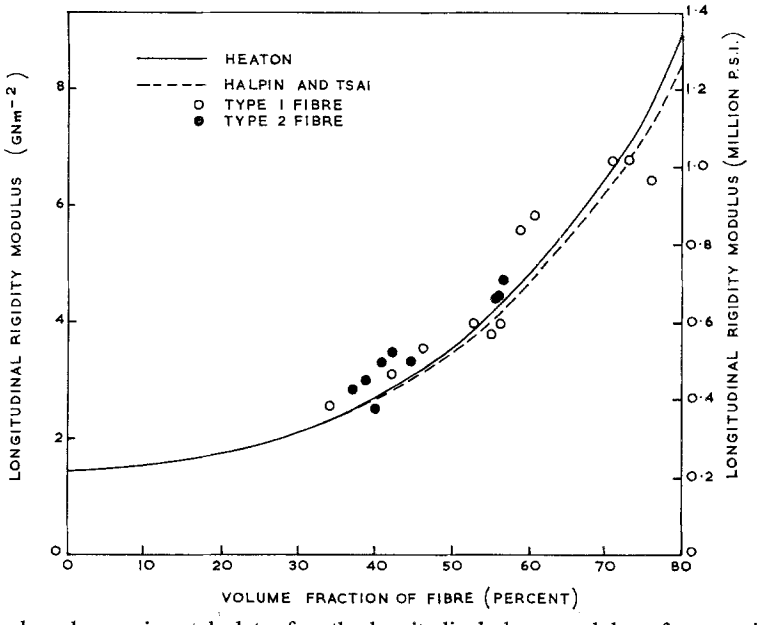

Figure 7 Theoretical and experimental data for the longitudinal shear modulus of composites of type 1 and type 2 fibre in resin system A.

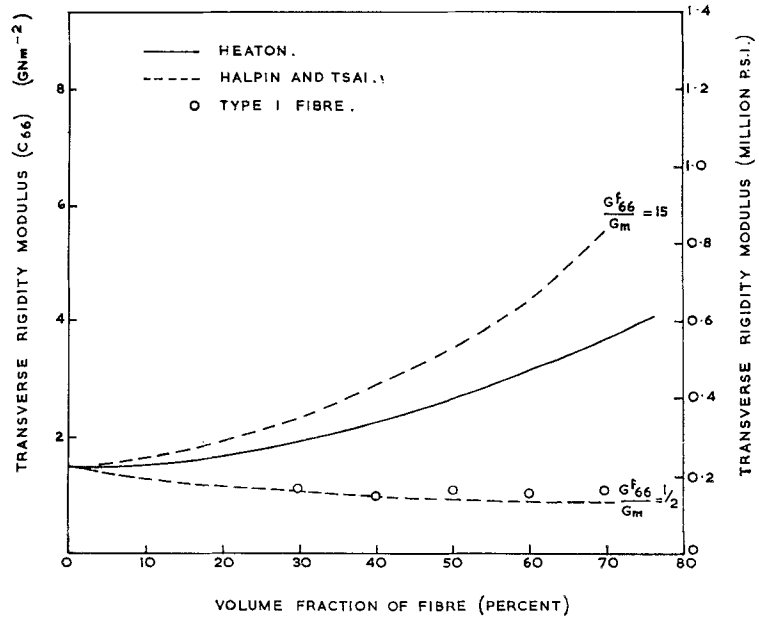

Figure 8 Theoretical and experimental data for the trans-verse shear modulus of composites of type 1 fibre in resin system A.

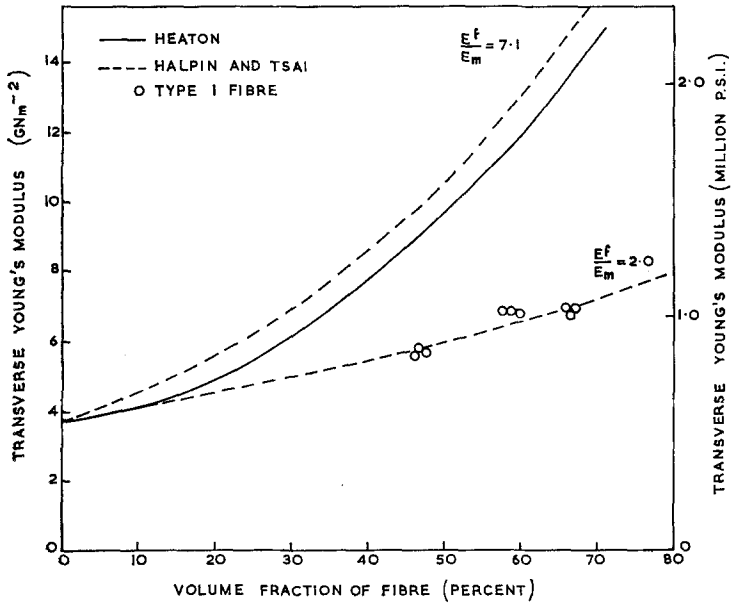

Figure 9 Theoretical and experimental data for the transverse Young's modulus of composites of type 1 fibre in resin system A.

torsional measurements. It is therefore concluded that either the assumed fibre constants are wrong or the models fall down in the prediction of this modulus.

It is of interest to calculate the fibre elastic constants which would bring the theoretical calculations into agreement with the experimental data. In the case of the Halpin Tsai equations it is easy to alter the assumed values of the fibre constants. It is not possible to do this with the Heaton model. It was found that the value of C_{66} for the fibre had to be about half the rigidity modulus of the resin to give agreement between the predicted and experimental values. This revised value gives a compliance S_{66} for the fibre of 1380 TN^{-1} m^2 compared to the originally assumed value of 94 TN^{-1} m^2.

Fig. 9 shows the theoretical and experimental data for the transverse Young's modulus for type 1 fibre in resin system A. Again both the Heaton and Halpin-Tsai calculations give similar values for the composite modulus. However, the values obtained are too high when the original fibre constants are used. In this case the fibre transverse modulus must be decreased to about 7 GNm^{-2} in order to give good agreement between the theoretical calculations and the experimental data. The revised value of S_{11} for the fibre becomes 130 TN^{-1} m^{-2}. Combining this with the value of S_{66} obtained earlier it is found that S_{12} becomes $-$ 560 TN^{-1} m^{-2}. The revised value of S_{11} for the fibre is lower than generally assumed but it is perfectly reasonable for a graphitic structure and in the absence of any direct measurement there seems no reason to doubt its validity.The very high value transverse Poisson's ratio implied by the revised values for S_{12} is impossible to accept physically. It is quite easy to demonstrate that such a value leads to a negative value for the bulk modulus of the fibre. This obviously contravenes the laws of thermodynamics and the revised values must be wrong. This means that the models for calculating elastic constants of the composites cannot deal successfully with the transverse shear properties.

Fig. 10 shows the transverse shear and Young's modulus for composites made with type 2 fibre. It was not possible to use the Heaton calculations for these composites. The best fit between experimental and theoretical results was obtained when G_{66} of fibre was taken at 2.9 GNm^{-2} and E_{11} as 15.3 GNm^{-2}. This gave values for S_{11} of 65 TN^{-1} m^2, for S_{66} of 345 TN^{-1} m^2 and for S_{12} of $-$ 109 TN^{-1} m^2. Again these values for S_{12} are physically impossible, thus confirming the inability of the module to deal with the transverse shear properties of the composite.

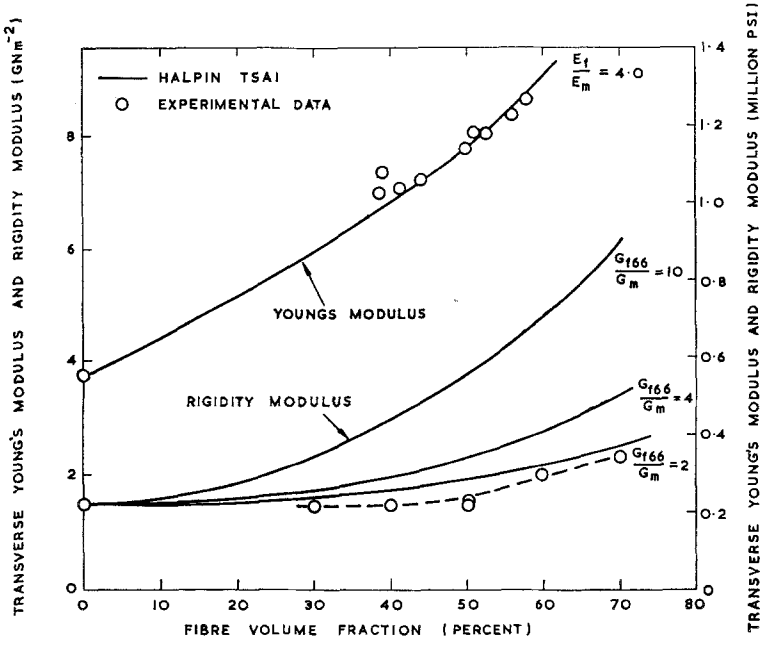

Figure 10 Theoretical and experimental data for the transverse shear modulus composites of type 2 fibre in resin system A, and the transverse Young's modulus of composites of type 2 fibre in resin system A.

It should be noted that the longitudinal Poisson's ratio is, according to the Halpin-Tsai equation, given by the law of mixtures. Since the composites were found to have similar Poisson's ratios to the resin this implies that the fibres also have a similar longitudinal Poisson's ratio. The values assumed for this fibre constant may therefore be revised to 0.33. This has the effect of altering S_{13} to 0.9 TN^{-1} m^2 for type 1 fibre and 1.6 TN^{-1} m^2 for type 2 fibre.

5. Conclusions

It has been found that the theoretical values of the elastic constants of unidirectional composites obtained from calculations based on different models are similar. In the case of carbon-fibre composites it was found that there was good agreement between the theoretical calculations and experimental data for those cases in which the fibre constants are known. The calculations of transverse Young's modulus and shear modulus gave answers which were too high with the generally assumed values of the relevant elastic constants of the fibre. These values are based on knowledge of the elastic properties of single crystals, and polycrystalline graphites.

On the assumption that the models for prediction of the elastic constants are correct, revised values for the elastic constants of the fibres can be estimated. These values contravene the laws of thermodynamics and therefore indicate that the models are wrong for the transverse shear properties.

Acknowledgements

The author wishes to thank Mr D. A. Stow who helped with some of the measurements reported here. He is also indebted to the Group under Mr H. Wells who manufactured the composites.

Appendix

Details of resin systems

System A	Parts by wt	Cure
Araldite resin MY 750	100	120°C for 3 h
Methylnadic anhydride (MNA)	80	
Benzyl dimethylamine (BDMA)	1	

System AV1		
Araldite resin MY 750	100	120°C for 3 h
Methylnadic anhydride	90	
Benzyl dimethylamine	1	
System AV2		
Araldite resin MY 750	100	80°C for 6 h, 125°C for 16 h
Methylnadic anyhdride	80	
Benzyl dimethylamine	1	
System AV3		
Araldite resin MY 750	100	80°C for 6 h, 125°C for 16 h
Methylnadic anhydride	90	
Benzyl dimethylamine	1	
System B		
Bakelite resin 19230	100	70°C for 12 h, 120°C for 4 h
Diaminodiphenylmethane	33	
System C		
Union Carbide 4617	116	120°C for 16 h, 165°C for 16 h
Metaphenylenediamine pre-impregnated from methyl-ethyl ketone solution	27	

References

1. C. KITTEL, "Introduction to Solid State Physics" (J. Wiley & Sons, New York) ch. 4.
2. G. RAMSDEN, *Brit. J. Non. Dest. Testing* **5** (1963) 101.
3. S. TIMOSHENKO and J. GOODIER, "Theory of Elasticity" (McGraw Hill, London and New York, 1951).
4. A. C. H. LOVE, "Mathematical Theory of Elasticity" (University Press, Cambridge, 1944).
5. C. C. CHAMIS and J. SENDECKYJ, *Comp. Mat.* **2** (1968) 332.
6. M. D. HEATON, *Brit. J. Appl. Phys.* (*J. Phys. D.*) Ser. 2 **1** (1968) 1039.
7. M. D. HEATON, *ibid* **3** (1970) 672.
8. J. C. HALPIN and S. W. TSAI, AFML-TR 67 423, (1969).
9. J. COOK, *Brit. J. Appl. Phys.* (*J. Phys. D.*) **1** (1968) 799.
10. P. EGELSTAFF, private communication.

Received 22 March and accepted 13 August 1972.